



City Research Online

City, University of London Institutional Repository

Citation: Silvers, L. J., Vasil, G. M., Brummell, N. H. & Proctor, M. R. E. (2009). Double-diffusive instabilities of a shear-generated magnetic layer. *The Astrophysical Journal Letters*, 702(1), doi: 10.1088/0004-637X/702/1/L14

This is the unspecified version of the paper.

This version of the publication may differ from the final published version.

Permanent repository link: <https://openaccess.city.ac.uk/id/eprint/1349/>

Link to published version: <https://doi.org/10.1088/0004-637X/702/1/L14>

Copyright: City Research Online aims to make research outputs of City, University of London available to a wider audience. Copyright and Moral Rights remain with the author(s) and/or copyright holders. URLs from City Research Online may be freely distributed and linked to.

Reuse: Copies of full items can be used for personal research or study, educational, or not-for-profit purposes without prior permission or charge. Provided that the authors, title and full bibliographic details are credited, a hyperlink and/or URL is given for the original metadata page and the content is not changed in any way.

Submitted for Publication in The Astrophysical Journal

Double-diffusive instabilities of a shear-generated magnetic layer

Lara J. Silvers

*Department of Applied Mathematics & Theoretical Physics, University of Cambridge,
Cambridge CB3 0WA, UK*

Geoffrey M. Vasil

JILA, University of Colorado, Boulder, CO 80309-0440

Nicholas H. Brummell

Dept. of Applied Mathematics & Statistics, University of California, Santa Cruz, CA 95064

Michael R.E. Proctor

*Department of Applied Mathematics & Theoretical Physics, University of Cambridge,
Cambridge CB3 0WA, UK*

ABSTRACT

Previous theoretical work has speculated about the existence of double-diffusive magnetic buoyancy instabilities of a dynamically-evolving horizontal magnetic layer generated by the interaction of forced vertically-sheared velocity and a background vertical magnetic field. Here, we confirm numerically that if the ratio of the magnetic to thermal diffusivities is sufficiently low then such instabilities can indeed exist, even for high Richardson number shear flows. Magnetic buoyancy may therefore occur via this mechanism for parameters that are likely to be relevant to the solar tachocline, where regular magnetic buoyancy instabilities are unlikely.

Subject headings: hydrodynamics — MHD — Sun: magnetic fields

1. Introduction

The generation of magnetic field by velocity shear and the field’s subsequent evolution are of great importance to an understanding of the operation of the solar dynamo. While the current dynamo paradigm contains many complex interacting components (see e.g. Parker (1993); Rempel (2006)), an integral part of all current large-scale solar dynamo models is the creation of strong toroidal magnetic structures in the tachocline, the Sun’s thin region of strong radial differential rotation separating the latitudinally differentially rotating convection zone and the solid-body-rotating radiative interior. Strong toroidal magnetic field is thought to be induced by the stretching action of the differential rotation on any background poloidal field (the Ω -effect of mean-field dynamo theory; Steenbeck et al. (1966)). Subsequently, magnetic buoyancy instabilities (Parker 1955) of the generated field are invoked as the mechanism for the creation of distinct magnetic structures and their subsequent rise toward eventual emergence at the solar surface as active regions.

In recent papers, Vasil & Brummell (2008, 2009) (hereinafter VB1, VB2) show that, when naively using the commonly accepted paradigm for the Ω -effect, it is surprisingly difficult to initiate magnetic buoyancy instabilities if thermodynamic adjustments are assumed to be adiabatic. Specifically, they concluded from analytic (VB2) and numeric (VB1) calculations that for magnetic buoyancy instabilities to operate in a thin tachocline, the velocity shear flow imposed to drive the system must be necessarily hydrodynamically unstable. Roughly speaking, VB2 found that $Ri \simeq \Delta z/H_p$ is required for magnetic buoyancy, where Ri is the Richardson number, Δz is the vertical shear width and H_p is the local pressure scale height. For the solar tachocline, the estimated Richardson number is very large ($Ri \simeq 10^3$ – 10^5) but the region is thin so that $\Delta z/H_p < 1$ (Gough 2007) and so the above condition for instability is therefore unlikely to be satisfied. The simulations of VB1 confirmed numerically that hydrodynamically unstable imposed shear flows could generate magnetic buoyancy instabilities in a thin shear region, but stable shear flows did not. Energetically, this can be thought of as the following conundrum; for magnetic buoyancy to occur, the shear flow must transfer enough energy into a toroidal magnetic field for it to overcome the stable background stratification. If the shear can only build (through an Alfvénic process) magnetic field to the level of equipartition with the flow, and the shear is constrained by the stratification (since it is hydrodynamically stable), then it is difficult for the shear-induced magnetic field to overcome the constraints of the stratification.

It is the case, however, that near the bottom of the convection zone the ratio between the magnetic and thermal diffusivities, $\zeta = \eta/\kappa$, is very small. It has long been recognized (Gilman 1970; Acheson 1979) that, in such circumstances, instabilities can occur that rely on the much greater diffusion rate of the stabilizing thermal component (see Hughes (2007)

for further discussions). Further, VB2 noted that instability might be enhanced by double-diffusive effects. Assuming isothermal (as opposed to adiabatic) adjustments VB2 obtained the much less stringent requirement that $\zeta Ri \simeq \Delta z/H_p$. It is therefore possible that a more-solar-like (high Ri) shear-generated magnetic field can become buoyantly unstable in a double-diffusive manner when $\zeta \ll 1$.

In this letter, we consider this possibility in a convectively stable atmosphere. We show that if ζ is sufficiently small, and the background Alfvénic timescales are sufficiently slow, then double-diffusive instabilities can exist for parameters that are relevant to the solar interior.

2. Equations and parameters

We consider a Cartesian domain (x, y, z) , where z is depth, x is the toroidal/zonal direction, and (y, z) are the poloidal directions. Our system consists of an initially vertical uniform magnetic field, $B_{z,0}$, permeating a stratified layer of compressible fluid under the influence of a forcing designed to generate a target shear flow $\mathbf{u} = (U_0(z), 0, 0)$. This system is similar to that described in VB1 and in Silvers *et al.* (2009). We solve standard non-dimensionalized equations for forced compressible magnetohydrodynamics governing the evolution of velocity $\mathbf{u} = (u, v, w)$, magnetic field $\mathbf{B} = (B_x, B_y, B_z)$, density ρ , temperature T , and pressure P based around a polytropic atmosphere, $T_0(z) = 1 + \theta z$, $\rho_0(z) = T_0(z)^m$, $P_0(z) = T_0(z)^{m+1}$. The non-dimensionalization uses T_* , the temperature at the top of the domain, ρ_* which is proportional to the total mass within the domain, $P_* = (c_p - c_v)T_*\rho_*$, the fiducial pressure (given the specific heat capacities, c_p, c_v), $B_{z,0}$, the imposed background magnetic field strength, the layer depth d , and time units of $\tau_* = d\rho_*^{1/2}/P_*^{1/2}$. We impose stress-free velocity and vertical magnetic field boundary conditions at $z = 0, 1$ together with $T(z = 0) = 1$ and $\partial_z T(z = 1) = \theta$. The horizontal directions are periodic.

The system is solved in a domain with aspect ratio 2:1:1 in a similar manner to that in VB1 and in Silvers *et al.* (2009) at a resolution of (roughly) $256 \times 256 \times 512$. This aspect ratio is specified to allow for certain expected dynamics, e.g. we anticipate three-dimensional modes to have smaller scales in the y and z directions than in the x direction. The thinness of the forced shear region compared to the local scale height is the geometrical factor that identifies the model with the tachocline. The kinetic and magnetic Reynolds numbers for our calculations are roughly $Re \sim 2000$, $Re_M \sim 1000$, respectively (based on the forced shear magnitude and width). Estimates of the numerical degrees of freedom (Davidson 2004) imply that our resolution is reasonable. However, we further satisfied ourselves that the results were consistent at varying resolutions.

The important parameters in the problem are the dimensionless thermal diffusivity, $C_K = K\tau_*/\rho_*c_p d^2$, the Prandtl number $\sigma = \mu c_p/K$ (μ representing dynamic viscosity), the inverse Roberts number $\zeta = \eta c_p \rho_*/K = \eta/\kappa$, and $\alpha = B_{z,0}^2 \tau_*^2 / \mu_0 \rho_* d^2$ which gives a measure of the Alfvén speed along the background field in terms of the fundamental acoustic velocity scale. Note that ζ is the critical parameter governing double-diffusive instability (Hughes & Weiss 1995).

We add a forcing term, $\mathbf{F} = -\sigma C_K \partial_z^2 U_0 \hat{\mathbf{x}}$, in the x -momentum equation that would (in the absence of magnetic effects and instabilities) maintain a desired target velocity $\mathbf{u} = (U_0(z), 0, 0)$ against viscous decay. We choose

$$U_0(z) = \frac{1}{20} \tanh \left[10 \left(z - \frac{1}{2} \right) \right] \quad (1)$$

to mimic the smooth radial shear transition believed to exist in the solar tachocline. The width is chosen sufficiently narrow that $\partial_z U_0 \approx 0$ (to within numerical precision) at the boundaries.

An important derived parameter is the Richardson number,

$$Ri = \min_{0 \leq z \leq 1} \left(\frac{N_0(z)^2}{[\partial_z U_0(z)]^2} \right), \quad (2)$$

where $N_0(z) = [-g \partial_z \ln (P_0(z)^{1/\gamma} / \rho_0(z))]^{1/2}$ is the local Brunt-Väisälä frequency of the stable background atmosphere, $\partial_z U_0(z)$ is the local turnover rate of the background shear and $\gamma = c_p/c_v = 5/3$. Ri measures the relative tendency of a shear flow to overturn fluid vertically compared to gravity's tendency to restore it to its original position. A large Ri implies that gravity is strongly stabilizing whereas a small value can mean that shear instabilities are possible (Drazin & Reid 2004). The goal in this work is to obtain a magnetic buoyancy instability at *high* Richardson number, a result not found in VB1, but here we investigate the low ζ regime where the effects of thermal stability are severely reduced.

While the Richardson number provides a useful rough measure of the stability properties of our system, we also define the respective thermal and magnetic Rayleigh numbers

$$R_T(z) = -\frac{N_0(z)^2}{\nu(z)\kappa(z)} \quad (3)$$

$$R_B(z) = \frac{g\alpha B_x(z)^2}{\nu(z)\kappa(z)P_0(z)} \frac{d}{dz} \ln B_x(z), \quad (4)$$

where $\kappa(z) = C_K/\rho_0(z)$, and $\nu(z) = \sigma\kappa(z)$. These definitions are consistent with those given in Hughes & Weiss (1995) except that here the magnetic Rayleigh number, R_B , is given in a

form that anticipates three-dimensional instabilities (Newcomb 1961). For the direct (non-oscillatory) type of instability, of interest here, both Rayleigh numbers are negative, and this corresponds to a thermal stratification that is stabilizing and magnetic gradient that is destabilizing. A Rayleigh number based on the total density stratification would correspond to $R_{\text{total}} = R_T - R_B$. The key result of VB2, derived under the adiabatic thermal adjustment assumption, is equivalent to saying that R_{total} is always negative (ostensibly stable) unless $Ri \ll 1$. In the double-diffusive context, where thermal adjustments are closer to isothermal, the critical parameter is actually $R_{\text{DD}} = R_T - \zeta^{-1}R_B$, where $\zeta \ll 1$. It is R_{DD} that is relevant to the stability of our system and it can potentially become positive even if $Ri \gg 1$. This is equivalent to the isothermal result derived in VB2 that required $\zeta Ri \simeq \Delta z/H_p$.

For the basic thermal parameters (see Table 1), we take the polytropic index $m = 1.6$ that enforces a convectively stable background polytropic stratification, and a non-dimensional lower-boundary heat flux of $\theta = 5$. With the chosen shear flow, this produced a minimum Richardson number of $Ri = 2.96$. While this value is significantly lower than we expect for the solar tachocline, it is high enough to guarantee that $U_0(z)$ hydrodynamically stable. This fact was checked numerically with a purely hydrodynamic run.

In order to see if double-diffusive instabilities can exist, we ran two simulations that differ *only* in the thermal diffusivity $\kappa = K/c_p\rho_*$ (varied through its non-dimensional counterpart C_K). Thus ζ and σ are varied commensurately to maintain fixed viscous and magnetic diffusivities $\mu = \sigma C_K$ and $\eta = \zeta C_K$. We keep $\sigma C_K = 2.5 \times 10^{-6}$ and $\zeta C_K = 5.0 \times 10^{-6}$ for all our cases. For our first case, C1, anticipating instability, we choose $\zeta = 5.0 \times 10^{-4}$, $\sigma = 2.5 \times 10^{-4}$ and $C_K = 0.01$. In our second case, C2, anticipating stability, we choose $\zeta = 0.01$, $\sigma = 5.0 \times 10^{-3}$ and $C_K = 5.0 \times 10^{-4}$. Thus, ζ in C1 is 20-fold smaller than in C2.

The parameter $\alpha = \sigma \zeta C_K^2 Q$ (where Q is the Chandrasekhar number measuring the ratio of magnetic and diffusive timescales) sets the background vertical magnetic field strength. For C1 and C2 we set $\alpha = 1.25 \times 10^{-5}$. We desire $\alpha \ll 1$ so that Alfvén timescales are slow compared to the acoustic timescale, and $Q \gg 1$ so that Alfvén timescales are fast compared to diffusion. C1 and C2 have $Q = 1.0 \times 10^6$. It turns out that the Alfvén timescale of the background magnetic field has important consequences for the *dynamic* stability of our evolving MHD configuration. To investigate this aspect, we therefore present a third case, C3, that is identical to C1 except that $\alpha = 5.0 \times 10^{-5}$, ($Q = 4.0 \times 10^6$). C3 therefore has two-fold faster Alfvén timescales.

3. Results

In all three simulations, we begin with a purely vertical magnetic field, and allow the induction of a toroidal field layer by the action of the imposed velocity forcing. In the absence of two- and three-dimensional effects, this induction process is governed by a one-dimensional (mean) set of MHD equations:

$$\rho_0(z)\partial_t u = \alpha\partial_z B_x + \sigma C_K \partial_z^2 u - \sigma C_K \partial_z^2 U_0 \quad (5)$$

$$\partial_t B_x = \partial_z u + \zeta C_K \partial_z^2 B_x. \quad (6)$$

Strictly speaking, the density profile in Equation (5) will evolve along with the shear flow and magnetic field. However, unlike the work in VB1-2 and Silvers *et al.* (2009), the target shear flow here, $U_0(z)$, has a *large* Richardson number. To an excellent approximation, the background density maintains its initial polytropic profile $\rho(t, z) = \rho_0(z)$ in this initial phase. The evolution, as shown in Figure 1, of the mean toroidal magnetic field is therefore essentially independent of the thermal properties of the system, unless two- or three-dimensional instabilities occur.

As time progresses, the peak field grows in the region of maximum forced velocity shear, and the field gradients strengthen. The ultimate question is whether a weak shear ($Ri > 1$) can induce strong enough gradients for a magnetic buoyancy instability to occur. Below, we show that two initially identically evolving one-dimensional MHD configurations can have completely different stability properties, based solely on the magnitude of the thermal diffusivity.

In C1, the system does indeed initially evolve according to Equations (5) and (6). However, since $\zeta = 5.0 \times 10^{-4}$ is small enough, the induction of mean toroidal field only proceeds for a finite time before an instability becomes apparent at $t \approx 88$. Figure (2) shows volume-rendered images at this time of the vertical velocity $w(x, y, z)$ and the fluctuating toroidal magnetic field $B_x(x, y, z) - \overline{B}_x(z)$. In the initial induction phase (governed by Equations (5) and (6)) both these quantities are zero. However, Figure (2) clearly shows that a wave-like perturbation in the vertical velocity and toroidal field has appeared in the region of strong toroidal magnetic field gradients near the top of the evolving toroidal magnetic layer. The instability appears in a quasi-two-dimensional manner with a wavevector primarily in the $y-z$ plane, taking a form that is similar to a classical ‘interchange’ instability (Cattaneo & Hughes 1988). Roll-like motions principally swap lines of toroidal magnetic field that pierce $y-z$ planes without a large degree of bending along the toroidal x -direction. There is a high degree of correlation between vertical velocity and toroidal field perturbations, strongly implying a buoyancy-driven instability (also see Figure 3).

We now compare C2 results with those of C1, which differs only the value of ζ . We

estimate the value of ζ for C2 to be sufficiently large to render R_{DD} everywhere negative, and therefore anticipate that the instability found in C1, if double-diffusive, should not appear in this case. We run C2 for over twice the time that it takes for the instability in C1 to manifest (up to $t \approx 180$) and the system simply continues to evolve according to the mean Equations (5) and (6). Eventually, these dynamics are benignly disrupted by Alfvénic processes without any buoyancy instabilities (as explained in VB2) and we therefore halt the computation. We conclude that the instability discovered in C1 is of a double-diffusive nature, since it depends critically on a sufficiently large thermal diffusivity (small ζ).

A subtle issue in this problem is the influence of the strength of the imposed background field. As argued in VB1-2, this essentially provides a timescale for disruptive Alfvénic processes. For instability to occur, the necessary conditions must be met before Alfvénic processes can disrupt the source. In VB1-2, this required a *strong* velocity shear (hydrodynamically unstable, $Ri \approx 0.03$) in order to induce the required magnetic gradients sufficiently quickly for a regular (mean-density-deficit driven) magnetic buoyancy instability to occur. Things are more complex in the high Ri , double-diffusive regime considered here. To elucidate this issue, we examine case C3 where the imposed background field strength is twice that of C1 and C2. Figure (3) shows a vertical profile of the mean vertical transport of B_x for both C1 and C3, a good indicator of the existence and efficiency of any magnetic buoyancy instabilities. The measure plotted is

$$C(z) = \frac{\overline{wB_x} - \overline{w}\overline{B_x}}{\max_z |w_{\text{rms}}B_{x,\text{rms}}|}, \quad (7)$$

where the overline represents a horizontal average, and $w_{\text{rms}}(z) = \sqrt{\overline{w^2} - \overline{w}^2}$, $B_{x,\text{rms}}(z) = \sqrt{\overline{B_x^2} - \overline{B_x}^2}$. For ease of comparisons, the normalization factor in the denominator for all cases is that value calculated for C1 and B_x is rescaled to the same units. Figure (3) shows that the toroidal magnetic field perturbations correlate well with vertical velocity perturbations, confirming that the instabilities are most likely of a magnetic buoyancy type. However, the dotted curve in this figure shows that the transport is significantly weaker for C3 in the initial stages of the instability. This is a signature of the dynamic nature of the instability. Owing to the evolving background state, R_{DD} does not entirely determine stability. In the equilibrium stability problem for quasi-incompressible motion without an imposed shear considered in Hughes & Weiss (1995), the growth rate of the instability becomes positive when $R_{\text{DD}} \geq 27\pi^4/4$. In the current problem, the portion of the domain that is unstable is perpetually moving as the magnetic layer evolves. Therefore, a locally unstable perturbation may not have enough time to amplify to a dynamically significant magnitude before it finds itself outside of the moving region of instability. Only if the growth rate of the instability is sufficiently large can an unstable mode amplify fast enough that the background appears effectively steady. Therefore, to exhibit instability in this evolving system unambiguously,

the growth rate of the instability must be at least of the order of the Alfvénic evolution timescale for the background,

$$p_{\text{crit}}(R_T, R_B, \sigma, \zeta) \approx \Delta z \sqrt{\sigma \zeta Q}, \quad (8)$$

where, $p_{\text{crit}}(R_T, R_B, \sigma, \zeta)$ is the maximal growth rate as a function of the Rayleigh numbers as given in Hughes & Weiss (1995), and the Chandrasekhar number $Q \gg 1$. Equation (8) implies that in the presence of a stronger background field, the instability requires a faster growth rate to proceed in the same manner. Even though C3 has the exact same background $\overline{B}_x(z)$ configuration as that for C1, the stronger background field strength, $B_{z,0}$, alters the nature of the instability. At the location where C1 grows strongly, C3 only reaches small amplitude (albeit in a shorter time: $t \approx 44$ cf. $t \approx 88$). However, the instability in C3 can still grow to significant amplitudes *higher up* in the domain as the system evolves further, as shown by the dashed curve in Figure (3). The amplitude is further modified since the stable background density stratification, and therefore R_{DD} changes slightly with height.

We have demonstrated that the presence of shear-generated double-diffusive magnetic buoyancy instabilities can be controlled primarily by the single parameter ζ . Given the dynamic nature of the instability here, the second most important parameter is the Chandrasekhar number, Q , which dictates the background Alfvénic timescales. C3 provides good evidence that the efficiency of the instability is governed through a relation at least qualitatively similar to Equation (8). However, the question remains as to whether any other parameters, such as the magnetic Prandtl number, $\sigma_{\text{M}} = \sigma/\zeta$, are critical to this process. Numerical constraints restrict our simulations to $\sigma_{\text{M}} = 0.5$, which is less than unity thus preserving the correct ordering of timescales, but larger than the estimated solar value of $\sigma_{\text{M}} \approx 6 \times 10^{-2}$ (Gough 2007). To make some progress, we extend the analysis of Hughes & Weiss (1995), noting again that this discusses the double-diffusive instabilities of an equilibrium rather than a dynamically-evolving system. It can be shown that Equation (8) embodies the solution to a 12th-order polynomial in p_{crit} . In the limit $\sigma, \zeta \ll 1$ and $R_T \ll 0$ this can be simplified to a cubic polynomial depending solely on the reduced variables $r = R_{\text{DD}}/|R_T|$, $q = \Delta z^2 Q/|R_T|$, and σ_{M} :

$$4X_r^3 + X_q X_r^2 - 18X_q X_r - X_q(27 + 4X_q) = 0, \quad (9)$$

where

$$X_q = \frac{q(1 + \sigma_{\text{M}})^3}{\sigma_{\text{M}}^2}, \quad X_r = \frac{(r - q)(1 + \sigma_{\text{M}})}{\sigma_{\text{M}}}. \quad (10)$$

Figure (4) shows the resulting dependence of the critical value of r versus q for several values of σ_{M} . In particular, it can be seen that the instability is more easily obtained for

smaller σ_M , which makes sense in terms of the lessening relative importance of viscosity, and, encouragingly, supports the viability of this process at more realistic solar parameters.

The transport measure $\overline{wB_x} - \overline{w}\overline{B_x}$ has a more complicated dependence on σ_M . In the appropriate Rayleigh number regime, $\overline{wB_x} - \overline{w}\overline{B_x} \sim p_{\text{crit}} + k_{\text{crit}}^2$, where k_{crit} is the horizontal wavenumber of the fastest growing mode. As σ_M is decreased, k_{crit} decreases and p_{crit} increases, and hence the dependence on σ_M is not straightforward. However, in the limit as $\sigma_M \rightarrow 0$, then $\overline{wB_x} - \overline{w}\overline{B_x} \sim p_{\text{crit}}$, which, from Figure (4), is nonzero even at $\sigma_M = 0$. This argument implies that, if we were able to run a computation at a significantly lower value of σ_M than in C1 and C3 (an extreme numerical challenge given our other parameters), we might expect that the buoyant transport should decrease, but not disappear altogether.

4. Conclusions

After the pessimistic results of VB1-2, it is encouraging that when double-diffusive effects are taken into account, the dynamics intuitively expected in the tachocline appear to be possible, satisfying the constraints that we have anticipated. We know roughly that $\zeta \approx 10^{-5}$ and $Ri \approx 10^3 - 10^5$ in the tachocline, and it is therefore plausible that their product is smaller than $\Delta z/H_p \approx 1$ (Gough 2007). However, we know very little about the configuration of any magnetic field in the solar tachocline or the associated Alfvénic timescales, and hence we do not know exactly *how much* smaller ζ must be for the growth rate of an instability to become large enough for it to proceed.

Even if instability occurs, it still remains unclear whether the nonlinear evolution of the system can produce magnetic fields that are sufficiently strong and coherent to be able to rise through the turbulent convection zone. While it now seems possible that high Ri shear flows could produce buoyant magnetic structures in the tachocline, one might expect that such buoyant structures would have magnetic energies that are (at most) in equipartition with the shear. If the turbulent convection zone acts locally in maintaining the tachocline’s shear, then it is difficult to see how magnetic structures could obtain the significantly greater strengths that are required to survive the disrupting effects of the convection zone (Tobias et al. 2001; Cline 2003; Fan et al. 2003). Of course, this question depends critically on how the energy of the shear relates to that of the convection zone, which is not well understood.

REFERENCES

Acheson, D.J. 1979, Sol. Phys., 62, 23

- Cattaneo, F. & Hughes, D.W. 1988, *J. Fluid. Mech.*, 196,323
- Cline, K.S. 2003, *The Formation and Evolution of Magnetic Structures in the Solar Interior*, PhD Thesis, University of Colorado
- Davidson, P.A. 2004, *Turbulence* (Oxford: Oxford University Press)
- Drazin, P.G. & Reid, W.H. 2004, *Hydrodynamic Stability* (2nd ed.; Cambridge: Cambridge University Press)
- Gilman, P.A., *ApJ*, 162, 1019.
- Gough, D.O. 2007, in *The Solar Tachocline*, eds. D.W. Hughes & R. Rosner, & N.O. Weiss (Cambridge: Cambridge University Press) 3
- Fan, Y. & Abbett, W.P. & Fisher, G.H. 2003, *ApJ*, 582, 1206
- Hughes, D. W. 2007, in *The Solar Tachocline*, eds. D.W. Hughes & R. Rosner, & N.O. Weiss (Cambridge: Cambridge University Press) 275.
- Hughes, D. W., & Weiss, N.O. 1995, *J. Fluid Mech.*, 301, 383
- Newcomb, W.A. 1961, *Phys. Fluids*, 4, 391
- Parker, E.N. 1993, *ApJ*, 408, 707
- Parker, E.N. 1955, *ApJ*, 122, 293
- Rempel, M. 2006, *ApJ*, 647, 662
- Silvers, L.J., Bushby P.J., & Proctor, M. R. E. 2009, *MNRAS*, in press (arXiv ref 0907.5068v1)
- Steenbeck, M. & Krause, F. & Rädler, K.H. ,1966, *Z. Naturf.*, 21a, 369
- Tobias, S.M. & Brummell, N.H. & Clune, T.L. & Toomre, J. 2001, *ApJ*, 549, 1183
- Vasil, G.M. & Brummell, N.H. 2008, *ApJ*, 686, 709
- Vasil, G.M. & Brummell, N.H. 2009, *ApJ*, 690, 2009, 783

Table 1. Parameters for Simulations

Case	ζ	σ	C_K	α	Q	Stability
C1	5.0×10^{-4}	2.5×10^{-4}	1.0×10^{-2}	1.25×10^{-5}	1.0×10^6	unstable
C2	1.0×10^{-2}	5.0×10^{-3}	5.0×10^{-4}	1.25×10^{-5}	1.0×10^6	stable
C3	5.0×10^{-4}	2.5×10^{-4}	1.0×10^{-2}	5.0×10^{-5}	4.0×10^6	delayed onset

Note. — In all cases, $m = 1.6$, $\theta = 5$, and $Ri_{\min} = 2.96$

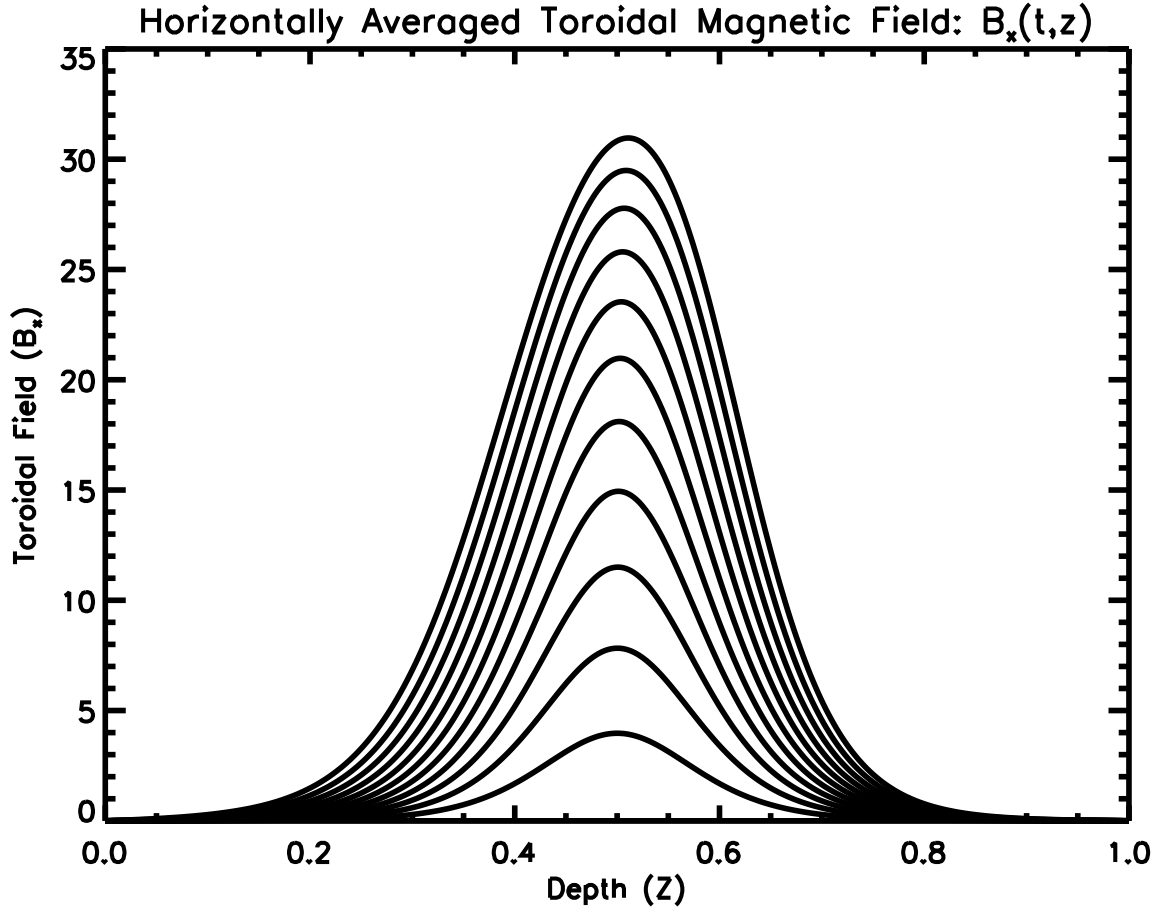


Fig. 1.— Time evolution of growing mean toroidal magnetic field vs. depth for C1 and C2. The field is initially zero and builds a growing peak that ends at $t \approx 88$.

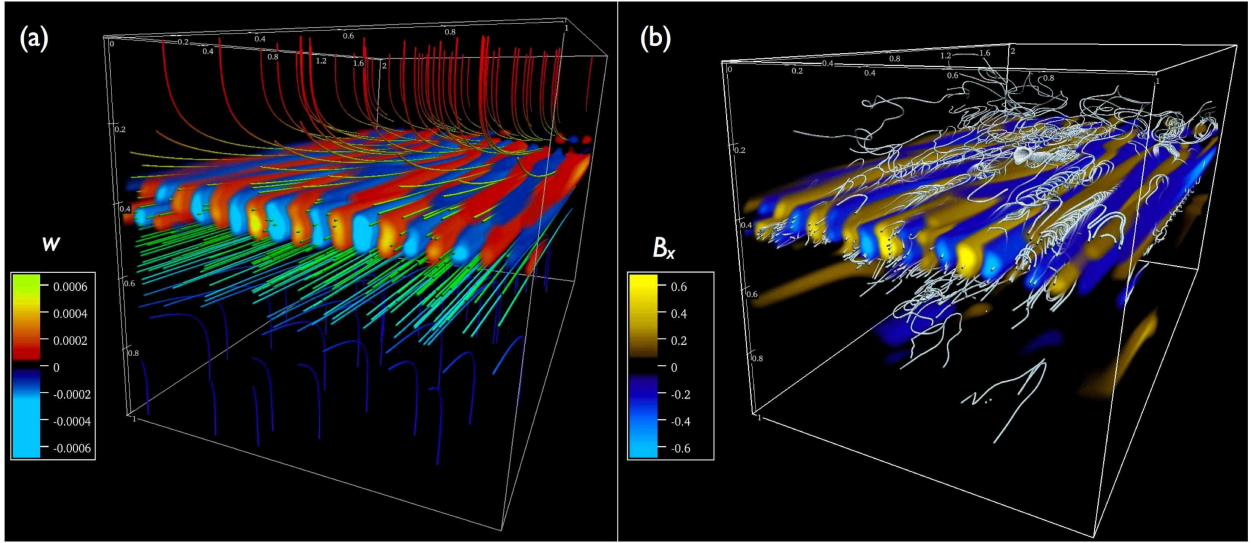


Fig. 2.— Volume-rendered images of flow and magnetic field from C1 at $t \approx 88$. Image (a) shows vertical velocity, $w(x, y, z)$ together with lines of magnetic field colored according to zonal velocity $u(x, y, z)$ (red tones near the top of the box indicate flow of one direction, blue tones near the bottom of the box indicate opposite flow, and green tones indicate approximate stagnation). Image (b) shows fluctuating toroidal magnetic field, $B_x(x, y, z) - \overline{B}_x(z)$. The silver lines indicate streamlines of the fluctuating velocity $(u - U_0, v, w)$.

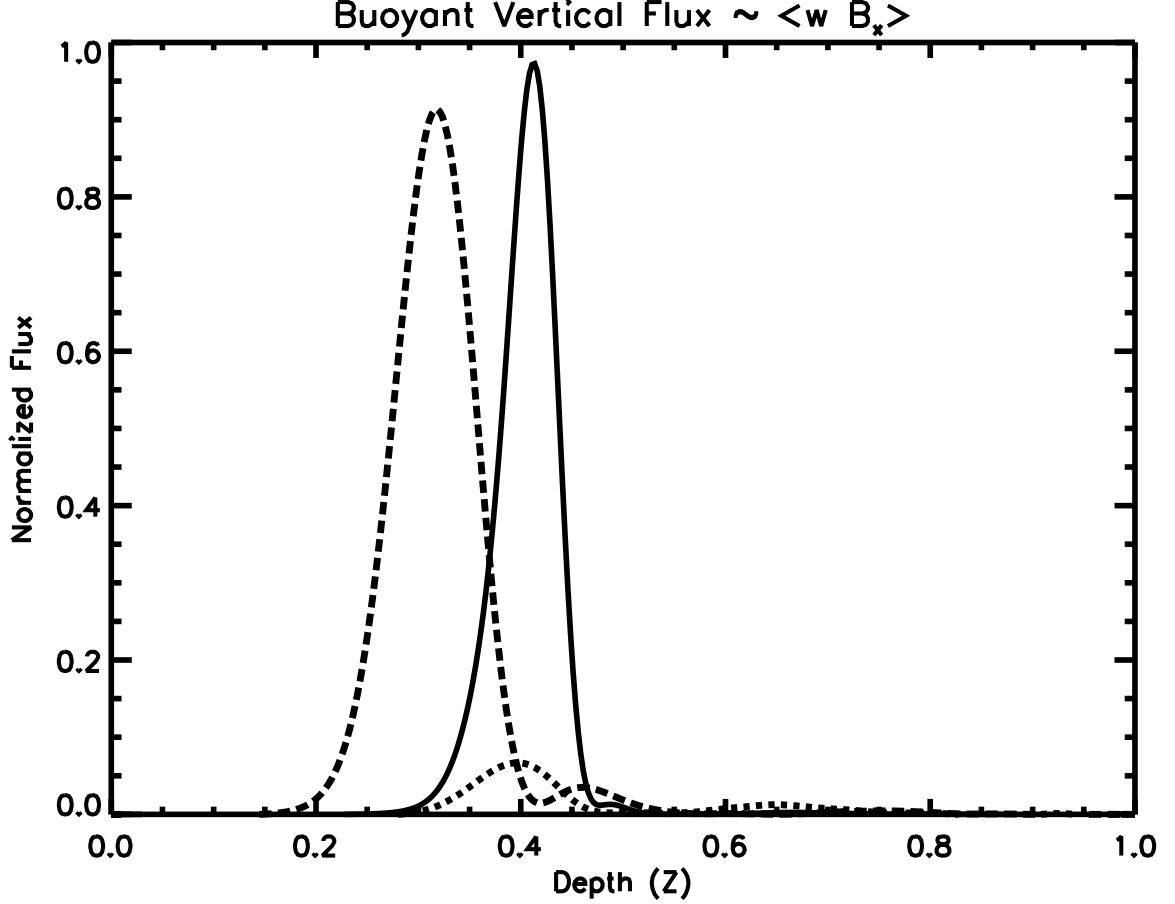


Fig. 3.— Normalized buoyant vertical flux vs. depth for C1 (solid) and C3 (dotted or dashed). All plots are proportional to $\overline{wB_x} - \overline{w}\overline{B_x}$ for each simulation and are scaled to be in the same units (B_x rescaled, and all normalized by the same constant value $(\max_z [\left(\overline{w^2} - \overline{w}^2\right) (\overline{B_x^2} - \overline{B_x}^2)]^{1/2}$ from C1). Since the Alfvén timescales are twice as fast, the C3 plots are shown both when the instability is occurring in the same vertical location as C1 (dotted, $t \approx 44$) and at the same actual time as the C1 plot (dashed, $t \approx 88$).

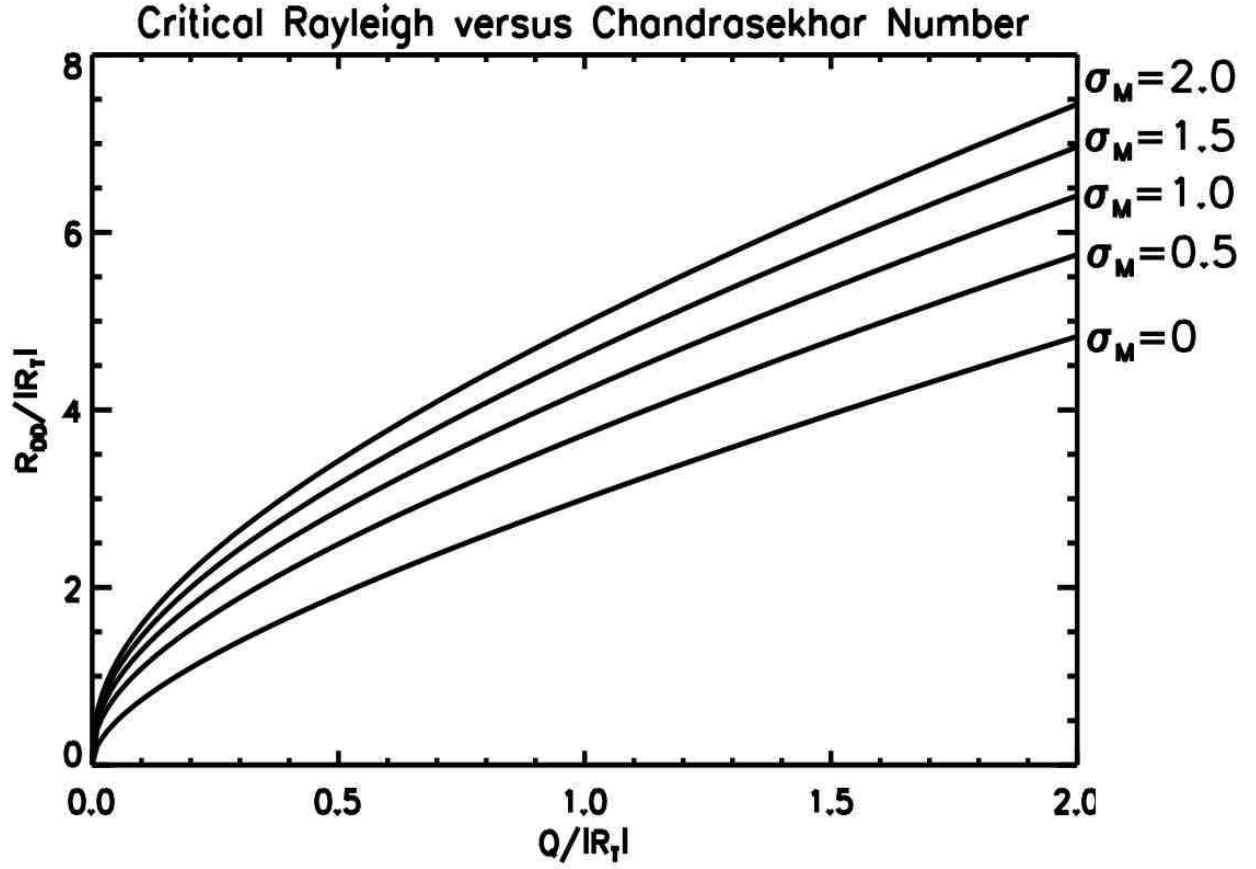


Fig. 4.— Critical $R_{DD}/|R_T|$ vs. $Q/|R_T|$ for $\sigma_M = \sigma/\zeta = 0, 0.5, 1.0, 1.5, 2.0$, in the limits $\sigma, \zeta \ll 1$, and $R_T \ll 0$.